

<https://doi.org/10.1038/s42003-024-07439-0>

# Proteolysis targeting chimera (PROTAC)-driven antibody internalization of oncogenic cell surface receptors



Ezequiel J. Tolosa<sup>1</sup>, Lin Yang<sup>1</sup>, Jennifer Ayers-Ringler<sup>1</sup>, Shinichiro Suzuki<sup>1</sup>, Jayapal Reddy Mallareddy<sup>2</sup>, Janet Schaefer-Klein<sup>1</sup>, Mitesh Borad<sup>3</sup>, Farhad Kosari<sup>1</sup>, Amarnath Natarajan<sup>2</sup> & Aaron S. Mansfield<sup>1</sup> ✉

Antibody-drug conjugates (ADCs) are increasingly used in clinic for multiple indications and may improve upon the activity of parental antibodies by delivering cytotoxic payloads into target cells. This activity is predicated upon internalization to release the cytotoxic payloads intracellularly. Since binding of ADCs to their cell surface targets does not guarantee their internalization, we hypothesize that proteolysis targeting chimeras (PROTACs) could improve the activity of ADCs through forced internalization. We show that PROTACs improve internalization of antibodies or their derivative antibody drug conjugates when both agents target the same oncogenic cell surface proteins (EGFR, HER2 or MET) by 1.4–1.9 fold in most models. PROTACs also significantly enhance cytotoxicity with HER2-targeting ADCs. These effects depend on dynamin and proteolysis. This application of PROTACs may impact the use of ADCs and provides a rationale to combine these agents in clinical trials.

Novel applications of proteolysis targeting chimeras (PROTACs) could improve the activity of antibody-drug conjugates (ADCs). Targeted protein degradation with PROTACs represents a novel strategy to eliminate oncogenic targets<sup>1,2</sup>. PROTACs are heterobifunctional molecules that consist of two protein-binding molecules that are bound by a linker. One protein-binding molecule recognizes a target, and the other recruits an E3 ubiquitin-protein ligase. By recruiting E3 ubiquitin-protein ligases to ubiquitylate target proteins, PROTACs result in signaling the proteasome to degrade these target proteins. PROTACs can recruit E3 ligases that typically do not ubiquitylate the target proteins as part of normal homeostasis. Whereas most research on PROTACs has focused on their direct effects on their targets, we hypothesized that PROTACs could enhance the internalization and cytotoxicity of ADCs through targeted degradation of the same oncogenic cell surface proteins.

Multiple ADCs have been approved by the FDA for treatment of solid tumors or hematologic malignancies, and others are in development<sup>3</sup>. ADCs are thought to improve the therapeutic index by selectively delivering potent cytotoxic payloads to tumor cells. One ADC, trastuzumab-deruxtecan (Tmab-deruxtecan), highlights how ADCs can improve upon the activity of the parent antibody. Whereas the parent antibody Trastuzumab (Tmab) is only effective against breast cancers with moderate to high levels of HER2 expression, the ADC Tmab-deruxtecan improves survival in patients whose

tumors have low levels of HER2 expression<sup>4</sup>. This finding suggests that the targeted delivery of the deruxtecan payload improves upon the efficacy of the parent antibody alone. Thus, this ADC has expanded the activity of the parent HER2-targeting antibody beyond the canonical HER2 biomarker-defined group of breast cancer.

Despite the success of Tmab-deruxtecan and the other ADCs, there are still limitations with this treatment modality related to (1) the premature deconjugation of the payload into systemic circulation with degradation of the linker, resulting in the diffusion of free payload into non-malignant tissues, (2) the formation of long-lived albumin linker payload adducts that form with linkers that react with the cysteine residues of serum albumin possibly causing off-target toxicity, (3) the internalization of ADCs through the Fcγ receptors (FcγR) on macrophages and other cells that bind to the Fc domain of the ADCs and are subsequently harmed by internalization and payload release<sup>5</sup>, and (4) the lack of localization of antibodies at the tumor target. Prior work has suggested that only 0.1% of tumor-targeting antibodies actually reach the tumor<sup>6</sup>. These issues with minimal on-target delivery and off-target toxicity are a major challenge and highlight the need to continue to optimize this promising therapeutic modality.

There is an additional limitation of ADCs that has not been extensively investigated, and that is their slow or limited internalization which could reduce the chances of their payloads being released within tumor cells.

<sup>1</sup>Mayo Clinic, Rochester, MN, USA. <sup>2</sup>Eppley Institute for Cancer Research, University of Nebraska Medical Center, Omaha, NE, USA. <sup>3</sup>Mayo Clinic, Phoenix, AZ, USA. ✉e-mail: [mansfield.aaron@mayo.edu](mailto:mansfield.aaron@mayo.edu)

Target binding by an ADC does not necessarily result in the automatic internalization of the ADCs and their targets. Whereas others have proposed that inhibiting endocytosis and blocking antibody internalization could optimize antibody-dependent cellular cytotoxicity (ADCC) or complement-dependent cytotoxicity (CDC)<sup>7</sup>, internalization is needed to degrade the linkers and dissociate the payloads for them to act on their target cells.

Given the existing limitations of ADCs, novel approaches could improve their efficacy or therapeutic index that enhance delivery to their targets or payload release within tumor cells. As others suggest that only a small fraction of antibodies reach their intended tumor target<sup>6</sup>, and that internalization of ADCs at the tumor site could be limited, we hypothesized that PROTACs might improve the internalization of ADCs by tumor cells, potentially enhancing their cytotoxicity. More specifically, we hypothesized that proteasomal degradation spurred by PROTACs would drive the internalization of their respective cell surface receptors. In this current work, we sought to determine whether the targeted protein degradation driven by PROTACs could optimize the internalization and cytotoxicity of ADCs that recognize the same oncogenic cell surface proteins.

## Results

### Internalization of cell surface protein targeting antibodies

To determine whether antibodies targeting cell surface oncogenic proteins were internalized, cell lines that expressed HER2, EGFR, and MET were selected. HER2, EGFR, and MET are transmembrane receptors that have oncogenic activity in multiple malignancies. Antibodies, ADCs, small molecular inhibitors, and PROTACs have been developed for clinical or research use for all three of these targets. Internalization of antibodies specific for each of the cell surface targets, including trastuzumab for HER2, cetuximab for EGFR, and ABT-700 for MET, was observed in all cell lines (Fig. 1, Supplementary Fig. 1). The lapatinib-based PROTAC SJF1528<sup>8</sup> that degrades HER2 and EGFR, and the capmatinib-based PROTAC 48-284<sup>9</sup> that degrades MET, were selected to test the effects of targeted degradation on antibody internalization. The co-administration of PROTACs that target the same cell surface proteins that are recognized by their respective antibodies significantly increased (1.4–1.9 fold) internalization of the antibodies in all cell lines with strong target expression, and mildly increased internalization of EGFR (1.1 fold) in the A549 cell line with weak EGFR target expression (Fig. 1a–c, Supplementary Fig. 1).

### Magnitude of internalization relies on antibody and PROTAC concentrations, and degrader activity

Increasing concentrations of antibodies, with constant concentrations of their respective protein targeting PROTACs, resulted in greater internalization of these antibodies compared to the controls (Fig. 2a), suggesting that the targets were not saturated by the antibodies at the tested concentrations. Increasing concentrations of the PROTAC SJF1528 with constant concentrations of antibody significantly increased antibody internalization at each dose strongly for SKBR3 and mildly for BT-474 (Fig. 2b). A hook effect has been described with PROTACs where increasing concentrations separately saturate their targets and E3 ligases, reducing the formation of trimeric complexes that results in target ubiquitylation<sup>10</sup>. No hook effect has been reported with SJF1528 at concentrations higher than used herein<sup>1</sup>. To determine the significance of degradation on internalization, we tested a second lapatinib-based degrader molecule SJF1521 which favors EGFR degradation over HER2<sup>8</sup>, SJF0661 an inactive PROTAC due to an inverted stereocenter at the hydroxyl-proline group of the VHL ligand that was designed as negative control for a BRAF degradation<sup>11</sup> and 48-279 which is an inactive PROTAC that targets MET<sup>9</sup> on the internalization of trastuzumab for HER2 and ABT-700 for MET. The PROTAC SJF1521 which favors EGFR degradation, did not result in the same degree of trastuzumab internalization we observed with SJF1528 (Fig. 2c). Similarly, the inactive MET-targeting PROTAC 48-279 did not result in the same degree of ABT-700 internalization we observed with 48-248 (Fig. 2c). The inactive PROTAC SJF0661 also did not enhance antibody internalization compared

to DMSO with antibody control conditions (Fig. 2c). Furthermore, none of PROTACs assayed enhanced internalization of non-specific human IgG controls in the HER2 and MET models (Fig. 2c). Altogether, these results provide strong evidence that the internalization rate is largely modulated by the activity of the degrader and the concentrations of the antibody and the PROTAC.

### Dependence on endocytosis and proteolysis

To understand which process mediates antibody internalization upon exposure to PROTACs, we used the endocytosis inhibitors Dyngo-4a and Pitstop2. Dyngo-4a inhibits clathrin-mediated endocytosis through inhibition of dynamin GTPase activity. Pitstop2 blocks interactions between the amino-terminal domain of clathrin heavy chain and amphipysin<sup>12</sup> and inhibits clathrin-independent endocytosis<sup>13</sup>. The dynamin inhibitor Dyngo-4a delayed the internalization of Tmab with PROTAC SJF1528 in the HER2-positive breast cancer cell line BT-474, and reduced antibody internalization in HER2-positive breast cancer cell line SKBR3 compared to treatment without Dyngo-4a (Fig. 3a). Similar delay or reduction on antibody internalization was observed without SJF1528, when Dyngo-4a was administered to the DMSO and Tmab control conditions (Supplementary Fig. 2a). Pitstop2 had no effect on antibody internalization with PROTACs in these models (Supplementary Fig. 2b). In contrast, in the absence of SJF1528, there was a significant reduction in antibody internalization with the clathrin inhibitor Pitstop2 in the BT-474 cell line but not SKBR3 (Supplementary Fig. 2c). These results suggest that some basal rates of antibody internalization are more sensitive to inhibition of clathrin-independent endocytosis, whereas PROTAC-mediated antibody internalization is more sensitive to clathrin-dependent endocytosis. In addition, inhibitors of the Ubiquitin-like modifier-activating enzyme 1 (Uba1), TAK-243<sup>14</sup>, and PYZD-4409<sup>15</sup> were assessed on Tmab and anti-MET internalization in the presence of SJF1528 and 48-284 PROTACs, respectively. Both inhibitors showed significant reduction in antibody internalization suggesting that ubiquitylation is required for antibody internalization driven by PROTACs (Fig. 3b). Furthermore, there was time-dependent degradation of the heavy and light chains of intracellular immunoglobulins upon treatment with PROTACs that was reduced by the addition of the proteasome inhibitor MG132 (Fig. 3c, d and Supplementary Fig. 2d). These results suggest that antibody internalization with PROTACs is more dependent on dynamin than clathrin in these models, and that internalization results in degradation of the antibody by the proteasome.

### Enhanced cytotoxicity of ADC and PROTAC combinations

To determine the effects of PROTACs on the activity of ADCs, the HER2-positive breast cancer cell lines BT-474 and SKBR3 were treated with the ADC trastuzumab-DM1 (Tmab-DM1) and Tmab-Deruxtecan with and without the HER2-targeting PROTAC SJF1528. The addition of the PROTAC reduced cell viability across multiple antibody concentrations at multiple time points (Fig. 4a–c, Supplementary Fig. 3a–c). Also, organoids derived from HER2-positive patient-derived xenografts (PDX) were treated with Tmab-Deruxtecan with and without the HER2-targeting PROTAC SJF1528. The addition of SJF1528 improved the cytotoxicity of ADC compared to the ADC treatment alone (Fig. 4d). We also evaluated the effects of lapatinib on cell survival and observed that this inhibitor had a stronger cytotoxic effect than the lapatinib-based PROTAC SJF1528. However, unlike the observed improvement in cytotoxicity of the combination SJF1528 and Tmab-Deruxtecan, the addition of lapatinib to Tmab-Deruxtecan did not impact cytotoxicity (Fig. 4e), suggesting that proteolysis had a role in the increased cytotoxicity of the PROTAC and ADC combination.

## Discussion

In this work, we identified an application of PROTACs not previously reported to the best of our knowledge. We have demonstrated that PROTACs can promote the internalization of cell surface receptors, and that antibodies attached to those same cell receptors can be internalized through

this process. We observed this effect across multiple oncogenic cell surface receptors in cell lines derived from different types of cancer. Furthermore, we found that targeted degradation of HER2 with a PROTAC can improve the cytotoxicity of HER2-targeting ADCs in cell lines and organoid models.

Many cell surface receptors are thought to be degraded by the lysosome; however, previous work has demonstrated that there is a mandatory role for the proteasome in normal endocytosis and subsequent degradation. For example, the proteasome is required for degradation of the interleukin-2 receptor following engagement with interleukin-2<sup>16</sup>. Thus, the mechanism of receptor degradation can be receptor-, cell- or context-dependent. Ubiquitylation has been shown to target some cell surface receptors for lysosomal degradation<sup>17,18</sup> or

proteasomal degradation<sup>19,20</sup>. In our work, by harnessing PROTACs, we demonstrated we could drive internalization of the antibodies bound to EGFR, HER2, and MET. Other approaches have been developed to target the degradation of cell surface or soluble proteins such as sweeping antibodies<sup>21</sup>, lysosome-targeting chimeras<sup>22</sup>, and others<sup>23</sup>. Based on the target and the context of its expression, one approach for cell surface degradation could be favored over another.

The design of ADCs continues to evolve<sup>24</sup>. Many efforts have been made to improve the drug-to-antibody ratio, and the linker chemistry for release of the payload within the target cells rather than in circulation. In our opinion, less effort has been made to affect the mechanisms of antibody internalization and whether those could be enhanced to improve the

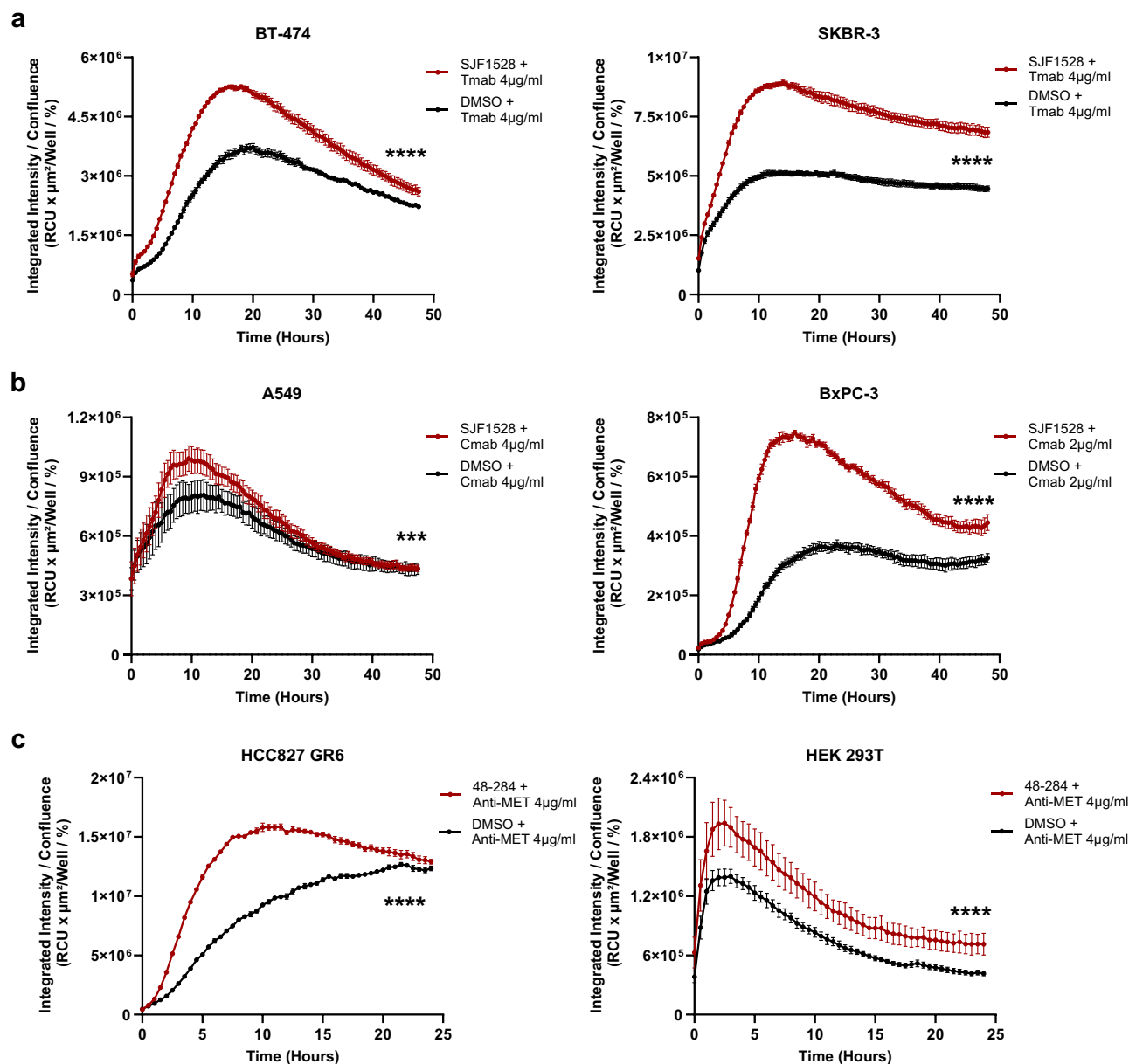


**Fig. 1 | PROTAC improves antibodies internalization targeting oncogenic tyrosine kinase receptors.** Cellular internalization of labeled antibodies was evaluated by in vitro live-cell imaging, plotted as AUC of Red integrated intensity over percentage of cell confluence as (RCU  $\times$   $\mu\text{m}^2$ /Well/%) in (a) breast cancer cell lines expressing HER2 (BT-474 and SKBR3) treated with PROTAC SJF1528 100 nM and Tmab at 4  $\mu\text{g}/\text{mL}$  compared against DMSO and Tmab at 4  $\mu\text{g}/\text{mL}$  control condition. b Lung (A549) and pancreatic (BxPC-3) cancer cells expressing EGFR treated with PROTAC SJF1528 100 nM and Cmab at 4  $\mu\text{g}/\text{mL}$  and 2  $\mu\text{g}/\text{mL}$ , respectively. c MET

cell models treated with PROTAC 48-284 500 nM and anti-MET antibody at 4  $\mu\text{g}/\text{mL}$  for HCC827 GR6 (Lung) and HEK 293T treated with PROTAC 48-284 500 nM and anti-MET antibody at 4  $\mu\text{g}/\text{mL}$ . Data shown here are representative experiments, every condition has been done in triplicate and lines and error bars represent the medians and SEM. Individual data points are available in the Supplementary Data file. Statistical significance was evaluated with GraphPad Prism 10 by unpaired *t*-test and two-tailed *p* value. \*\*\**P* < 0.001; \*\*\*\**P* < 0.0001.

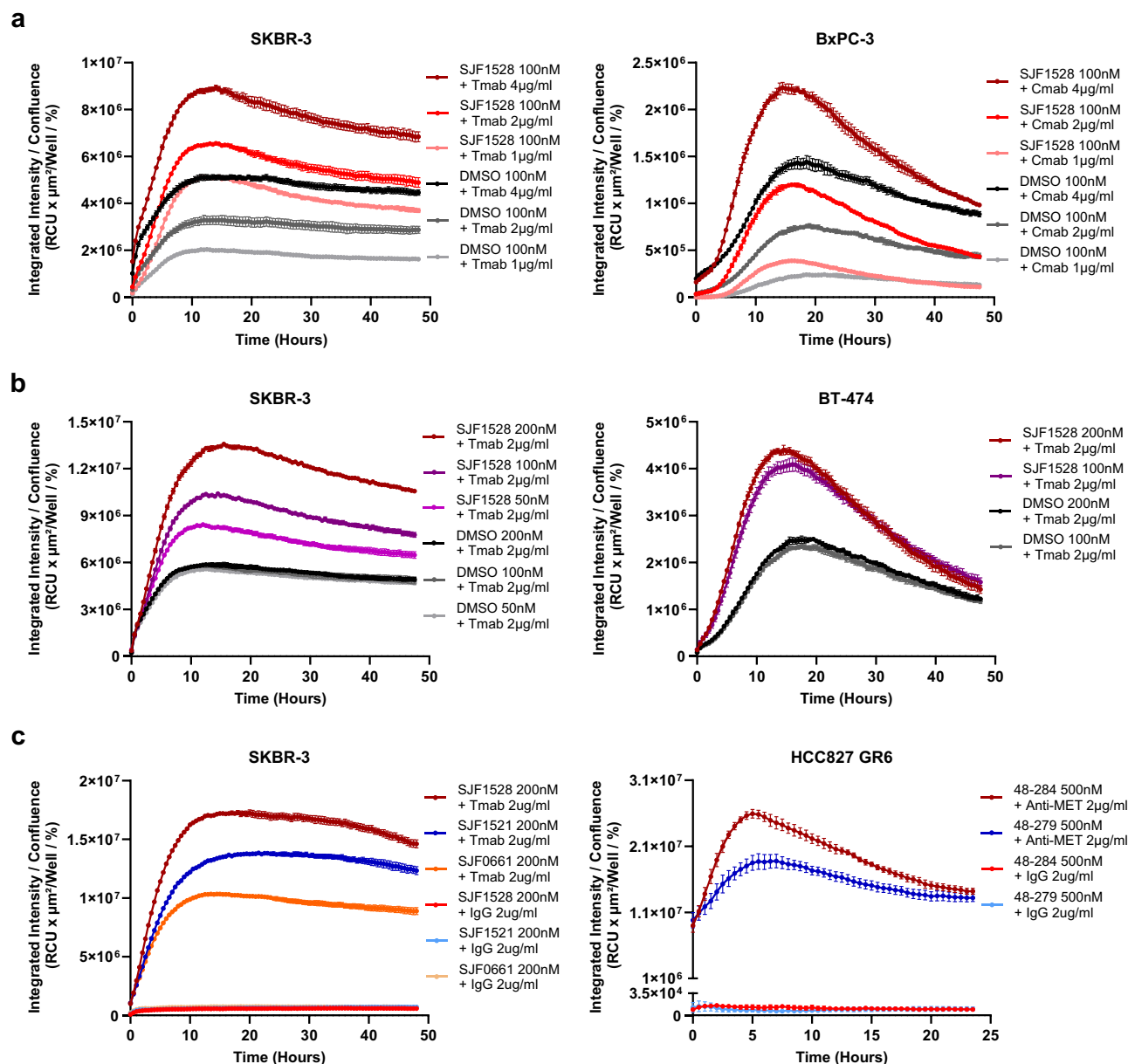


**Fig. 2 | Antibody internalization is antibody and PROTAC concentration dependent and relies on degrader target-specific activity.** Internalization of Tmab, Cmam, and anti-MET was evaluated by *in vitro* live-cell imaging, plotted as AUC (RCU x  $\mu\text{m}^2/\text{Well}$  / %) as previously described. **a** SKBR3 and BxPC-3 cell lines were treated with PROTAC SJF1528 100 nM and Tmab (4  $\mu\text{g}/\text{ml}$ , 2  $\mu\text{g}/\text{ml}$ , 1  $\mu\text{g}/\text{ml}$ ) or Cmam (4  $\mu\text{g}/\text{ml}$ , 2  $\mu\text{g}/\text{ml}$ , 1  $\mu\text{g}/\text{ml}$ ), respectively, and compared with the DMSO control conditions without PROTAC. **b** SKBR3 and BT-474 cells were treated with Tmab 2  $\mu\text{g}/\text{ml}$  and PROTAC SJF1528 at (200 nM, 100 nM, 50 nM) or (200 nM, 100 nM), respectively, and compared with DMSO control conditions without

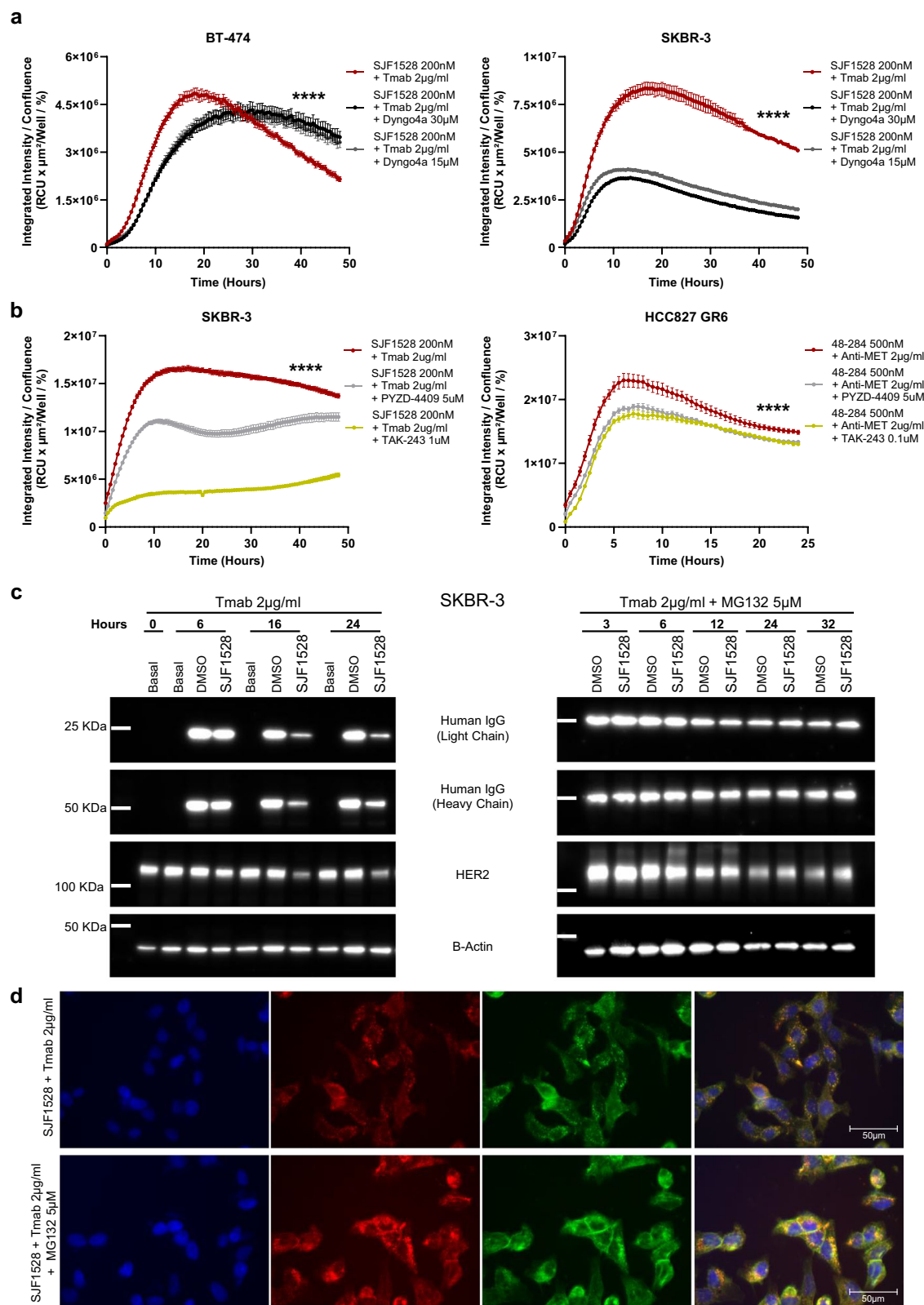
PROTAC. **c** SKBR3 cells were treated with Tmab or human IgG (2  $\mu\text{g}/\text{ml}$ ) and PROTAC SJF1528 (200 nM) or off-target antigen specificity PROTAC SJF1521 (200 nM) or the inactive degrader SJF0661 (200 nM). HCC827 GR6 cells were treated with anti-MET or human IgG (2  $\mu\text{g}/\text{ml}$ ) and PROTAC 48-284 (500 nM) and inactive degrader 48-279 (500 nM). Data shown here are representative experiments, every condition has been done in triplicate and lines and error bars represent the medians and SEM. Individual data points are available in the Supplementary Data file.

therapeutic index. It has been shown that both endocytosis and the intracellular accumulation of the payloads correlate with therapeutic efficiency of some ADCs<sup>25</sup>. To our knowledge most efforts to improve internalization utilized biparatopic antibodies that induce target cross-linking to increase internalization<sup>26,27</sup>. When there is low surface expression of the targets, cross-linking may not readily occur, possibly giving an advantage to combining ADCs with PROTACs to mediate internalization in this setting.

Many antibodies that are approved by the FDA for the treatment of cancers utilize the IgG1 subclass which is associated with strong ADCC and CDC. Others have proposed that inhibition of endocytosis optimizes the activity of ADCC-mediating antibodies<sup>7</sup>. In contrast, internalization is

typically required for the activity of ADCs, and binding of an antibody to its target does not necessarily trigger internalization. For these reasons, it is possible that enhancing the internalization of antibodies could improve the delivery of a conjugated payload, while minimizing ADCC and CDC. ADCs are hypothesized to selectively deliver payloads to target cells. Unfortunately, there is evidence that these therapies have off-target toxicities and unintended adverse effects due to the nature of their design. For instance, the linker between the antibody and the payload can bind albumin and prolong systemic exposure to the payload. Also, the heavy chain of the antibody can be recognized by Fc $\gamma$ R on macrophages or natural killer cells resulting in the uptake of the antibodies by those cells and the negative consequences of





payload release within these unintended target cells. Because of these off-target toxicities of ADCs, it might be beneficial to use lower doses of ADCs if their activity at the target site can be optimized. Although only supported by in vitro evidence at this time, our data support studying combinations of PROTACs with lower doses of ADCs to further optimize the therapeutic index.

In summary, we have demonstrated that PROTACs enhance the internalization of antibodies that target the same oncogenic cell-surface proteins as their respective PROTAC. Antibody internalization was sensitive to inhibition of dynamin and the proteasome. Ultimately, the activity of HER2-targeting ADCs was improved with PROTACs across a range of ADC concentrations over multiple time points. This application of

**Fig. 3 | Endocytosis and Uba1 inhibitors disrupt PROTAC induced-antibodies internalization and MG132 blocks internalized-antibody degradation.** Antibody internalization was evaluated in the presence of endocytosis inhibitors (Dyngo-4a and Pitstop2) and ubiquitin-proteasome system inhibitors (TAK-243, PYZD-4409, and MG132). **a** BT-474 and SKBR3 cells were assayed by in vitro live-cell imaging for Tmab internalization and PROTAC SJF1528 in presence of the dynamin mediated endocytosis inhibitor Dyngo-4a at (30 and 15  $\mu$ M). **b** SKBR3 and HCC827 GR6 cells were also assayed for Tmab or anti-MET internalization and PROTAC SJF1528 or 48-284, respectively, in presence of the Uba1 inhibitors TAK-243 and PYZD-4409. **c** Time course evaluation of the internalized Tmab by Western blots with antibodies specific against light and heavy human IgG chains and HER2 expression on SKBR3

cells treated with or without SJF1528 200 nM and Tmab 2  $\mu$ g/mL, and SJF1528 200 nM with Tmab 2  $\mu$ g/mL and MG132 5  $\mu$ M. **d** Representative images of immunofluorescence staining of BT-474 cells assayed overnight with SJF1528 200 nM and labeled Tmab 2  $\mu$ g/mL or SJF1528 200 nM with Tmab 2  $\mu$ g/mL, MG132 5  $\mu$ M and a secondary antibody for human IgG-FITC conjugated. Data shown here are representative experiments, every condition has been done in triplicate and lines and error bars represent the medians and SEM. Individual data points are available in the Supplementary Data file and the uncropped Western blots are in the Supplementary figures. Statistical significance was evaluated with GraphPad Prism 10 by unpaired *t*-test and two-tailed *p* value. \*\*\*\**P* < 0.0001.

PROTACs may impact the use of ADCs and provides a rationale to further study these combinations, possibly in clinical trials with further validation.

## Methods

### Cells and cell culture

Breast cancer cell lines (BT-474 and SKBR3 [both cell lines provided by Dr. Taro Hitosugi]), lung cancer cells (A549 [ATCC] and HCC827 GR6 [Sigma Aldrich]), and the pancreatic cancer cell line (BxPC-3 [ATCC]) were cultured in RPMI 1640 with L-glutamine (Corning 10-040-CV). HEK 293T (ATCC) cells were cultured in MEM (Gibco 11095-080) supplemented with 10% fetal bovine serum (Gibco 10437-028), 100 IU/mL penicillin, and 100  $\mu$ g/mL streptomycin (Gibco 15140-122) at 37 °C with 5% CO<sub>2</sub> in a humidified incubator.

### PROTACs 48-284 and 48-279

To develop MET-targeting PROTACs, capmatinib was linked to thalidomide, lenalidomide, and VHL binders, as described elsewhere<sup>9</sup>. The MET PROTAC 48-284 resulted in the strongest degradation of MET in the prior screen. In contrast, 48-279 had a shorter linker than 48-284 and was inactive<sup>9</sup>.

### 3D culture models

Organoids derived from PDX breast cancer models were generated as described below. Tumor tissues were minced into small pieces of 1–3 mm, transferred into the gentle MACS C tubes (Miltenyi Biotec 130-093-237) with DMEM medium (Corning 10-013-CV) without fetal bovine serum plus tumor dissociation kit (enzymes H, R and A) (Miltenyi Biotec 130-095-929) and digested for 1 h in gentleMACS dissociator (Miltenyi Biotec 130-093-235) according to the manufacturer recommendations. After dissociation, the cell suspensions were centrifuged and washed twice with DMEM medium and filtered with 40  $\mu$ m cell strainers (Falcon 352340) to remove not digested tissue. The single-cell suspensions were then subject to a negative selection with mouse cell depletion kit (Miltenyi Biotec 130-104-694) for 20 min at 4 °C and continuous rotation. Then magnetic separation with LS Columns (Miltenyi Biotec 130-042-401) was performed to enrich and recover the human breast tumor cells. Between 10,000 to 15,000 cells/well were seeded in 96-well suspension culture plates (Greiner Bio-One 655185) in DMEM medium supplemented with 10% fetal bovine serum (Gibco 10437-028), 1% glutamax (Gibco 35050-061), non-essential amino acids (Corning 25-025-CI), 100 IU/mL penicillin, 100  $\mu$ g/mL streptomycin (Gibco 15140-122) and 5  $\mu$ M of ROCK inhibitor (Tocris Bioscience 1254), and incubated for 7–10 days at 37 °C degrees with 5% CO<sub>2</sub> in a humidified incubator.

### Live-cell imaging and antibody internalization

All live-cell imaging experiments for antibody internalization were performed with IncuCyte S3-C2 (Sartorius Corporation). Cells were seeded at a density of 10,000 cells/well and 50  $\mu$ l of culture medium in black-walled 96-well plates (Corning CLS3603) and incubated overnight before treatment. PROTAC reagents targeting HER2 and EGFR SJF1528 (Tocris Bioscience 7262) or MET (48-284) were assayed in a range of concentrations (from 50 to 500 nM). Other PROTAC molecules such as SJF1521 (Tocris Bioscience

7261) that favor EGFR degradation over HER2, SJF0661 (Tocris Bioscience 7464) designed as negative control for a BRAF degrader and 48-279 targeting MET with no degradation activity were also assayed across a range of concentrations (from 200 to 500 nM). Trastuzumab (Tmab) (Med Chem Express HY-P9907), Cetuximab (Cmab) (Med Chem Express HY-P9905), anti-MET (Creative Biolabs ABT-700), and Human IgG1 (Sino Biological HG1K) antibodies were used at a final concentration of 1, 2, and 4  $\mu$ g/mL and labeled with Human FabFluor-pH red reagent (Sartorius Corporation 4722). A total of 50  $\mu$ l of antibody-dye mix was added to each well and four images per well were acquired every 30 min for at least 24 h with the adequate light channel following the manufacturer's recommendations. The quantitative data generated from these experiments were exported as Excel files and used to generate the AUC and statistical analysis on GraphPad Prism 10.

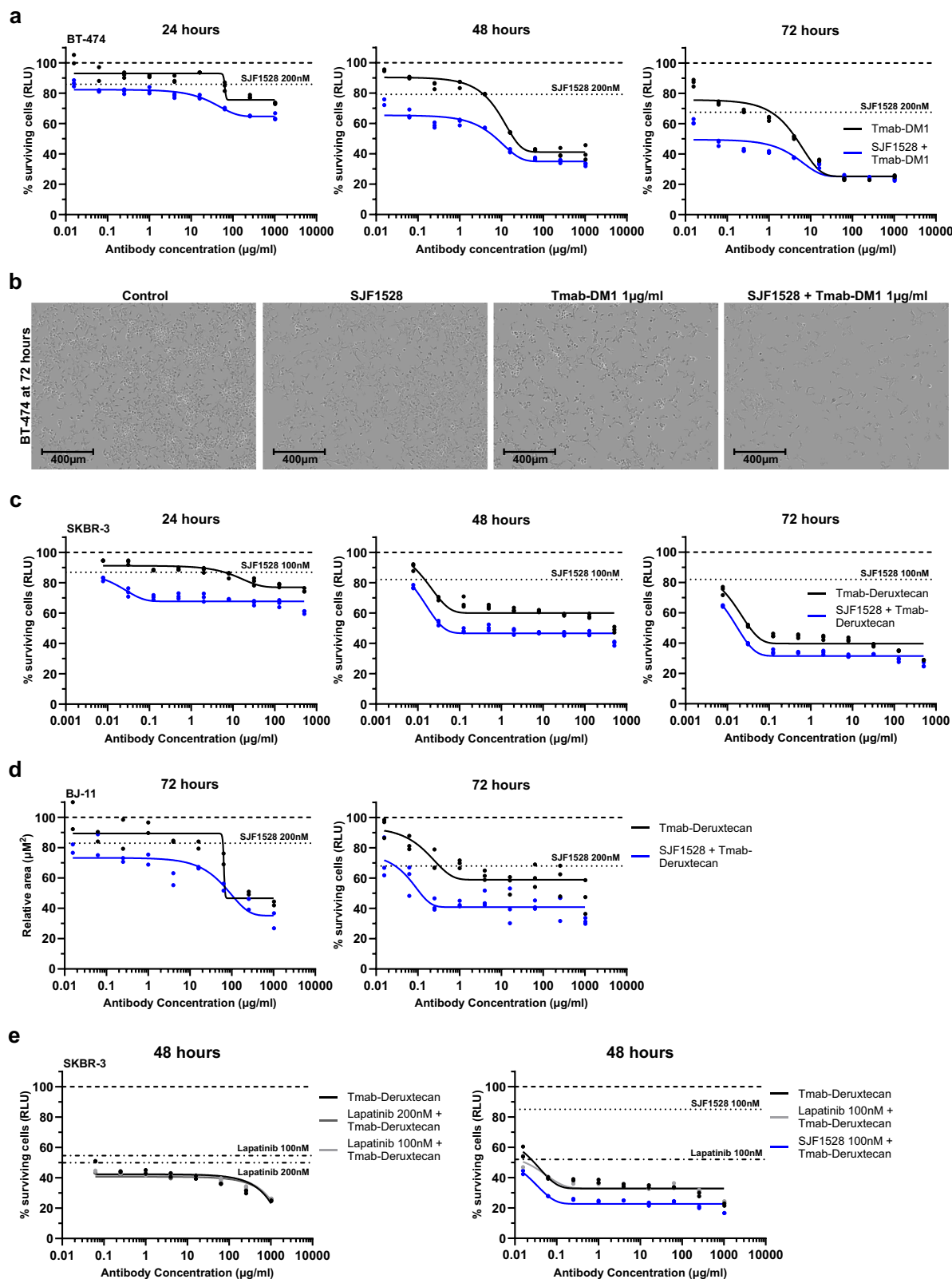
### Inhibition experiments

Antibody internalization was also evaluated in the presence of endocytosis and ubiquitin-proteasome system inhibitors. The breast cancer cell lines BT-474 and SKBR3 and the lung cancer cell line HCC827 GR6 were assessed for live-cell imaging as we described before. Both, the dynamin I/II or clathrin inhibitors Dyngo-4a and Pitstop2 (Med Chem Express HY-13863 and HY-115604, respectively) and Uba1 inhibitors TAK-243 and PYZD-4409 (Med Chem Express HY-100487 and HY-13297, respectively) were added to the cells at the same time that labeled antibodies Tmab and anti-MET were added, and internalization evaluated by acquiring images with IncuCyte every 30 min for 24–48 h as before.

Internalized antibodies were also tested by Western blots using primary antibodies detecting light and heavy chains (R&D Systems MAB100502 and MAB1101, respectively) derived from Human IgGs in BT-474 and SKBR3 cell lines treated with proteasome inhibitor MG132 (Selleckchem S2619). Cells were seeded at a density of 400,000 cells/well in 1.5 mL of culture medium in 6-well plates (Corning CLS3603) and incubated overnight at 37 °C before addition of antibody or PROTAC with antibody at different time points.

### Western immunoblots

Cells seeded and treated in 6-well plates as described before were washed 2–3 times with PBS (Corning 21-031-CV) and lysed with home-made NETN lysis buffer plus protease inhibitors cocktail (Roche 11836170001). Cell lysates cleared by centrifugation at 4 °C for 10 min at 15,000  $\times$  g and protein concentration was measured with Pierce BCA protein assay kit (Thermo scientific 23225) using the Promega GloMax Explorer plate reader. Equal amounts of proteins from cleared cell lysates were mixed with loading SDS buffer plus  $\beta$ -mercaptoethanol, resolved in 4–20% precast mini-protein gels (Bio-Rad 4561096), and transferred to PVDF membranes. Chemiluminescence was detected by the ChemiDoc digital imaging system after incubation with Pierce ECL western blotting substrate (Thermo Scientific 32106). Other primary antibodies used for immunoblotting were anti-HER2 (D8F12 Cell Signaling 4290), anti- $\beta$ -actin (BioLegend 643802), and anti-GAPDH (Santa Cruz Biotechnology sc-365062). Secondary antibodies used were goat anti-rabbit (Santa Cruz Biotechnology sc-2030) and mouse IgG kappa binding protein (Santa Cruz Biotechnology sc-516102).



## Immunofluorescence staining

Red Fabfluor-pH sensitive labeled Tmab was assayed by immunodetection after internalization overnight in BT-474 cells. A secondary anti-Human IgG (Fc specific)-FITC antibody (F9512 Millipore Sigma) was used for Human IgG detection. Briefly, 40,000 cells/well were seeded in the Millicell EZ Slide (C86024 Millipore Sigma) and incubated for 1 day.

After, SJF1528 and Red Fabfluor labeled Tmab (2  $\mu\text{g/mL}$ ) or SJF1528 and Red Fabfluor labeled Tmab (2  $\mu\text{g/mL}$ ) and MG132 (5  $\mu\text{M}$ ) were added and incubated overnight. The cells were fixed with 4% paraformaldehyde for 10 min at room temperature, permeabilized with Triton 0.1%, and blocked with 1% BSA and 22.5 mg/mL glycine in PBST for 1 h. The cells were then incubated with anti-Human IgG-FITC antibody for 1 h at

**Fig. 4 | PROTAC enhances the cytotoxic activity of ADCs.** Viability and proliferation were assayed on HER2-positive cells (BT-474 and SKBR3), and breast cancer organoids (BJ11) treated with PROTAC SJF1528 (at 200 or 100 nM) and a range of concentrations of Tmab-DM1 or Tmab-Deruxtecan, respectively. Also, lapatinib and lapatinib with Tmab-Deruxtecan combination were assayed with SKBR3 cells and with similar ADC concentrations as described before. The data are represented as percentage of surviving cells (RLU) or relative area ( $\mu\text{m}^2$ ), normalized to a non-treated control condition (DMSO). **a** Viability of BT-474 cells after 24, 48, and 72 h of treatment. **b** Representative images of BT-474 cells without treatment (DMSO) and treated with PROTAC SJF1528 200 nM only, Tmab-DM1 1  $\mu\text{g}/\text{mL}$  only, and the combination PROTAC SJF1528 200 nM and Tmab-DM1 1  $\mu\text{g}/\text{mL}$  at

72 h. **c** Viability of SKBR3 cells after 24, 48, and 72 h of treatment. **d** Representative graphs of independent experiments with breast cancer organoid (BJ11) showing relative area as measurement of proliferation rate in single organoids experimental setting and as percentage of surviving cells (RLU) with multiple organoids/well after 72 h of treatment. **e** Survival of SKBR3 cells assayed with lapatinib and the combinations of lapatinib and Tmab-Deruxtecan, and SJF1528 with Tmab-Deruxtecan for comparison. - - - - DMSO non-treated control; ..... PROTAC (SJF1528) treatment; · - · - · lapatinib at 100 nM and - · - · - lapatinib at 200 nM, respectively. Data shown here are representative experiments, every condition has been done in triplicate and lines and error bars represent the medians and SEM. Individual data points are shown.

37 °C in a humidified chamber, washed 3 times for 10 min each with PBS, and mounted with Doulink in situ counter staining media with DAPI (DUO82040 Sigma). Images were acquired with EVOS 5000 Imaging system and DAPI, using GFP and Cy5 light filter cubes (ThermoFisher Scientific).

### Cell lines viability assays

The effects of PROTAC and the ADC Kadcyla (trastuzumab-emtansine, Tmab-DM1) or Enhertu (trastuzumab-deruxtecan, Tmab-deruxtecan) on the viability of BT-474 and SKBR3 tumor cell lines was assessed with Cell Titer-Glo (Promega Corporation G7571). For live-cell imaging, cells were seeded at a density of 10,000 cells/well in 50  $\mu\text{L}$  of culture medium in black-walled 96-well plates (Corning CLS3603) and incubated overnight. Cells were then treated with different ADCs concentrations, PROTAC, or the combination of PROTAC and ADCs in separate experiments for 24, 48, and 72 h. Also, lapatinib (Med Chem Express HY-50898) alone and the combination of lapatinib with Tmab-deruxtecan effect on cell survival were evaluated on SKBR3 cells for comparison against lapatinib-based PROTAC SJF1528 with Tmab-deruxtecan combination. After the desired time, 100  $\mu\text{L}$  of Cell Titer-Glo reagent was added to each well, incubated at room temperature for 10–15 min, and luminescence measured with Promega GloMax Explorer. Dose-response curves were generated with GraphPad Prism 10 and four-parameter fitting curves (inhibitor vs response variable slope). Cells treated with DMSO only were used as control conditions to normalize the data.

### Organoids proliferation and viability

Deidentified organoids derived from PDX breast cancer models were provided by Mayo Clinic's BEAUTY program to the current team with only HER2 status shared. These organoids were collected under Mayo Clinic IRB approval following patient consent. These organoids were evaluated for proliferation by measuring the relative area ( $\mu\text{m}^2$ ) after treatment with PROTAC, Tmab-deruxtecan or the combination of PROTAC and Tmab-deruxtecan in a range of concentrations for 72 h. Briefly, single organoids were transferred with 30  $\mu\text{L}$  of culture medium into ultra-low attachment 96-well U-bottom plates (Corning 4520) and cultured overnight. Then, 30  $\mu\text{L}$  of culture medium and reagents were added to achieve the desired concentration and bright field images were taken at 10 $\times$  for further analysis. All the images were calibrated using Fiji to convert pixels into Micras, and after setting the measurements the freehand selection tool was used to draw the perimeter of at least three organoids per experimental condition. The quantitative data generated from these experiments were exported to Excel files and used to generate the graphs on GraphPad Prism 10 as relative area ( $\mu\text{m}^2$ ). DMSO control condition was used to normalize the data for other treatments (Fig. 4d).

Viability assays were also performed using multiple organoids per well. For these experiments, organoids were treated similarly to the cell line viability experiments described before. Briefly, organoids were cultured with 50  $\mu\text{L}$  of culture medium. Then, 50  $\mu\text{L}$  of different ADC concentrations, PROTAC, or the combination of PROTAC with ADC was added and treated for 72 h. Then 100  $\mu\text{L}$  of Cell Titer-Glo reagent was added to each well, shaken for 5 min, incubated at room temperature for 20 min, and

luminescence measured with Promega GloMax Explorer. Also, dose-response curves were generated with GraphPad Prism 10 and four-parameter fitting curves (inhibitor vs response variable slope) as described before. Organoids treated with DMSO only were used as control conditions to normalize the data.

### Statistics and reproducibility

The total area under the curves representing antibody internalization was determined using GraphPad from triplicates and compared between experimental groups with a two-tailed, unpaired *t*-test. The null hypothesis was that there would be no differences in antibody internalization between groups. There were no adjustments for multiple comparisons. To calculate fold changes, the areas under the curves of the experimental groups were divided by that of the control groups. The raw data obtained with IncuCyte, and the summary statistics we derived, are included in the Supplementary Data files, organized by figure and models, to improve reproducibility of our analyses.

### Reporting summary

Further information on research design is available in the Nature Research Reporting Summary linked to this article.

### Data availability

The primary data are summarized as per the results of this manuscript, and raw data are available in Supplementary Data file. The cell lines and antibodies can be purchased from vendors as listed. The MET PROTAC 48-284<sup>9</sup> is in limited supply and requires synthesis. The HER2-positive breast cancer organoid is a limited passage model which is not available for use beyond the current work. Please contact the corresponding author for any requests.

Received: 12 June 2024; Accepted: 23 December 2024;

Published online: 31 December 2024

### References

1. Burslem, G. M. & Crews, C. M. Proteolysis-targeting chimeras as therapeutics and tools for biological discovery. *Cell* **181**, 102–114 (2020).
2. Schapira, M., Calabrese, M. F., Bullock, A. N. & Crews, C. M. Targeted protein degradation: expanding the toolbox. *Nat. Rev. Drug Discov.* **18**, 949–963 (2019).
3. Tsuchikama, K., Anami, Y., Ha, S. Y. Y. & Yamazaki, C. M. Exploring the next generation of antibody-drug conjugates. *Nat. Rev. Clin. Oncol.* **21**, 203–223 (2024).
4. Modi, S. et al. Trastuzumab deruxtecan in previously treated HER2-low advanced breast cancer. *N. Engl. J. Med.* **387**, 9–20 (2022).
5. Tarantino, P., Ricciuti, B., Pradhan, S. M. & Tolane, S. M. Optimizing the safety of antibody-drug conjugates for patients with solid tumours. *Nat. Rev. Clin. Oncol.* **20**, 558–576 (2023).
6. Mach, J. P. et al. Tumor localization of radio-labeled antibodies against carcinoembryonic antigen in patients with carcinoma: a critical evaluation. *N. Engl. J. Med.* **303**, 5–10 (1980).



7. Chew, H. Y. et al. Endocytosis inhibition in humans to improve responses to ADCC-mediating antibodies. *Cell* **180**, 895–914 e827 (2020).
8. Burslem, G. M. et al. The advantages of targeted protein degradation over inhibition: an RTK case study. *Cell Chem. Biol.* **25**, 67–77 e63 (2018).
9. Mallareddy, J. R. et al. Fluorescence based live cell imaging identifies exon 14 skipped hepatocyte growth factor receptor (MET) degraders. *bioRxiv*, 2024.2011.2022.624922 (2024).
10. Casement, R., Bond, A., Craighan, C. & Ciulli, A. Mechanistic and structural features of PROTAC ternary complexes. in *Targeted Protein Degradation: Methods and Protocols* (eds Cacace, A. M., Hickey, C. M. & Békés, M.) 79–113 (Springer US, 2021).
11. Alabi, S. et al. Mutant-selective degradation by BRAF-targeting PROTACs. *Nat. Commun.* **12**, 920 (2021).
12. von Kleist, L. et al. Role of the clathrin terminal domain in regulating coated pit dynamics revealed by small molecule inhibition. *Cell* **146**, 471–484 (2011).
13. Dutta, D., Williamson, C. D., Cole, N. B. & Donaldson, J. G. Pitstop 2 is a potent inhibitor of clathrin-independent endocytosis. *PLoS ONE* **7**, e45799 (2012).
14. Hyer, M. L. et al. A small-molecule inhibitor of the ubiquitin activating enzyme for cancer treatment. *Nat. Med.* **24**, 186–193 (2018).
15. Xu, G. W. et al. The ubiquitin-activating enzyme E1 as a therapeutic target for the treatment of leukemia and multiple myeloma. *Blood* **115**, 2251–2259 (2010).
16. Yu, A. & Malek, T. R. The proteasome regulates receptor-mediated endocytosis of interleukin-2. *J. Biol. Chem.* **276**, 381–385 (2001).
17. Richardson, D. S., Gujral, T. S., Peng, S., Asa, S. L. & Mulligan, L. M. Transcript level modulates the inherent oncogenicity of RET/PTC oncoproteins. *Cancer Res.* **69**, 4861–4869 (2009).
18. Scott, R. P., Eketjall, S., Aineskog, H. & Ibanez, C. F. Distinct turnover of alternatively spliced isoforms of the RET kinase receptor mediated by differential recruitment of the Cbl ubiquitin ligase. *J. Biol. Chem.* **280**, 13442–13449 (2005).
19. Pierchala, B. A., Milbrandt, J. & Johnson, E. M. Jr. Glial cell line-derived neurotrophic factor-dependent recruitment of Ret into lipid rafts enhances signaling by partitioning Ret from proteasome-dependent degradation. *J. Neurosci.* **26**, 2777–2787 (2006).
20. Tsui, C. C. & Pierchala, B. A. The differential axonal degradation of Ret accounts for cell-type-specific function of glial cell line-derived neurotrophic factor as a retrograde survival factor. *J. Neurosci.* **30**, 5149–5158 (2010).
21. Igawa, T., Haraya, K. & Hattori, K. Sweeping antibody as a novel therapeutic antibody modality capable of eliminating soluble antigens from circulation. *Immunol. Rev.* **270**, 132–151 (2016).
22. Ahn, G. et al. Elucidating the cellular determinants of targeted membrane protein degradation by lysosome-targeting chimeras. *Science* **382**, eadf6249 (2023).
23. Wells, J. A. & Kumru, K. Extracellular targeted protein degradation: an emerging modality for drug discovery. *Nat. Rev. Drug Discov.* **23**, 126–140 (2024).
24. Tolcher, A. W. The evolution of antibody-drug conjugates: a positive inflexion point. *Am. Soc. Clin. Oncol. Educ. Book* **40**, 1–8 (2020).
25. Gera, N. et al. MYTX-011: a pH-dependent anti-cMET antibody-drug conjugate designed for enhanced payload delivery to cMET expressing tumor cells. *Mol. Cancer Ther.* **23**, 1282–1293 (2024).
26. Cheng, J. et al. Molecular mechanism of HER2 rapid internalization and redirected trafficking induced by anti-HER2 biparatopic antibody. *Antibodies* **9**, 49 (2020).
27. Li, J. Y. et al. A biparatopic HER2-targeting antibody-drug conjugate induces tumor regression in primary models refractory to or ineligible for HER2-targeted therapy. *Cancer Cell* **29**, 117–129 (2016).

## Acknowledgements

The authors are grateful to Bobbi Jebens for her administrative assistance with this manuscript. The PDX breast cancer models were supplied by the BEAUTY study which is funded in part by the Mayo Clinic Center for Individualized Medicine; Nadia's Gift Foundation; John P. Guider; the Eveleigh Family; George M. Eisenberg Foundation for Charities; generous support from Afaf Al-Bahar; and the Pharmacogenomics Research Network (PGRN). Other contributing groups include the Mayo Clinic Cancer Center and the Mayo Clinic Breast Specialized Program of Research Excellence (SPORE).

## Author contributions

Ezequiel J. Tolosa: conceptualization, methodology, formal analysis, investigation, writing. Lin Yang: methodology, formal analysis, investigation, writing. Jennifer Ayers-Ringler: methodology, formal analysis, investigation, writing. Shinichiro Suzuki: methodology, formal analysis, investigation, writing. Jayapal Reddy Mallareddy: resources, formal analysis, investigation, writing. Janet Schaefer-Klein: supervision, project administration, formal analysis, writing. Mitesh Borad: formal analysis, writing. Farhad Kosari: methodology, formal analysis, investigation, writing. Amar Natarajan: conceptualization, methodology, investigation, formal analysis, writing, Supervision. Aaron S. Mansfield: conceptualization, methodology, investigation, formal analysis, writing, supervision, funding acquisition.

## Competing interests

Mayo Clinic submitted patent 63/560,270 related to this work for the institution on 01 March 2024 listing the inventors Aaron S. Mansfield M.D., Ezequiel J. Tolosa Ph.D., Jennifer R. Ayers-Ringler Ph.D., Lin Yang Ph.D., and Farhad Kosari Ph.D. that is under review at the time of publication. Mitesh Borad reports grants to Mayo Clinic from Senhwa Pharmaceuticals, Adaptimmune, Agios Pharmaceuticals, Halozyne Pharmaceuticals, Celgene Pharmaceuticals, EMD Merck Serono, Toray, Dicerna, Taiho Pharmaceuticals, Sun Biopharma, Isis Pharmaceuticals, Redhill Pharmaceuticals, Boston Biomed, Basilea, Incyte Pharmaceuticals, Mirna Pharmaceuticals, Medimmune, Bioline, Sillajen, ARIAD Pharmaceuticals, PUMA Pharmaceuticals, Novartis Pharmaceuticals, QED Pharmaceuticals, Pieris Pharmaceuticals; and consulting to self from ADC Therapeutics, Exelixis Pharmaceuticals, Inspyr Therapeutics, G1 Therapeutics, Immunovative Therapies, OncBioMune Pharmaceuticals, Western Oncolytics, Lynx Group, Genentech, Merck, and Huya. Aaron Mansfield reports consulting fees to his institution from Genentech, Bristol Myers Squibb, AbbVie, AstraZeneca, Janssen, BeiGene, Takeda, Genzyme, Gilead Sciences, and Johnson & Johnson Global Services.

## Additional information

**Supplementary information** The online version contains supplementary material available at <https://doi.org/10.1038/s42003-024-07439-0>.

**Correspondence** and requests for materials should be addressed to Aaron S. Mansfield.

**Peer review information** *Communications Biology* thanks Mackenzie Krone, and the other, anonymous, reviewer for their contribution to the peer review of this work. Primary Handling Editors: Laura Rodríguez and Ophelia Bu. A peer review file is available.

**Reprints and permissions information** is available at <http://www.nature.com/reprints>

**Publisher's note** Springer Nature remains neutral with regard to jurisdictional claims in published maps and institutional affiliations.

**Open Access** This article is licensed under a Creative Commons Attribution-NonCommercial-NoDerivatives 4.0 International License, which permits any non-commercial use, sharing, distribution and reproduction in any medium or format, as long as you give appropriate credit to the original author(s) and the source, provide a link to the Creative Commons licence, and indicate if you modified the licensed material. You do not have permission under this licence to share adapted material derived from this article or parts of it. The images or other third party material in this article are included in the article's Creative Commons licence, unless indicated otherwise in a credit line to the material. If material is not included in the article's Creative Commons licence and your intended use is not permitted by statutory regulation or exceeds the permitted use, you will need to obtain permission directly from the copyright holder. To view a copy of this licence, visit <http://creativecommons.org/licenses/by-nc-nd/4.0/>.

© The Author(s) 2024